Modeling and Design of Die Profile of Extrusion of Square Section from Round Billet through Non-linear Converging Dies

A THESIS SUBMITTED IN PARTIAL FULFILMENT

OF THE REQUIREMENTS FOR THE DEGREE OF

Master of Technology

In

Mechanical Engineering

By

SANTOSH CHAUBEY

Department of Mechanical Engineering

National Institute of Technology

Rourkela (India)

2011

Modeling and Design of Die Profile of Extrusion of Square Section from Round Billet through Non-linear Converging Dies

A THESIS SUBMITTED IN PARTIAL FULFILMENT

OF THE REQUIREMENTS FOR THE DEGREE OF

Master of Technology

In

Mechanical Engineering

By

SANTOSH CHAUBEY

UNDER THE GUIDANCE OF

Prof. K P Maity

Department of Mechanical Engineering

National Institute of Technology

Rourkela (India)

Dedicated to

My Most

Loving Family

Acknowledgement

I express my deep sense of gratitude and indebtedness to my thesis supervisor Dr. K.P Maity, Professor, Department of Mechanical Engineering for providing precious guidance, inspiring discussions and constant supervision throughout the course of this work. His timely help, constructive criticism, and conscientious efforts made it possible to present the work contained in this thesis.

I express my sincere thanks to Mr. A.K Rout and Mr. L.N. Patra, Ph.D research scholars for some discussion. I am grateful to Prof. R. K. Sahoo, Head of the Department of Mechanical Engineering for providing me the necessary facilities in the department. I express my sincere gratitude to Prof. S.S. Mahapatra, coordinator of PG course for his timely help during the course of work. I am also thankful to all the staff members of the department of Mechanical Engineering and to all my well wishers for their inspiration and help. I express my sincere thanks to my classmate's Umesh Kumar vishwakarma, Matruprasad rout and Kamal Kumar kanaujia for their help during my project work.

I feel pleased and privileged to fulfill my parent's ambition and I am greatly indebted to them for bearing the inconvenience during my M Tech. course.

Date: Santosh Chaubey

Roll No. 209ME2196

National Institute of Technology

Rourkela (India)

CERTIFICATE

This is to certify that thesis entitled, **"MODELING AND DESIGN OF DIE PROFILE OF EXTRUSION OF SQUARE SECTION FROM ROUND BILLET THROUGH NON-LINEAR CONVERGING DIES**" submitted by **Mr. SANTOSH CHAUBEY** in partial fulfillment of the requirements for the award of Master of Technology in Mechanical Engineering with "Production Engineering" Specialization during session 2010-2011 in the Department of Mechanical Engineering National Institute of Technology, Rourkela.

It is an authentic work carried out by him under my supervision and guidance. To the best of my knowledge, the matter embodied in this thesis has not been submitted to any other University/Institute for award of any Degree or Diploma.

Date:

Dr. K. P. Maity

Professor

Department of Mechanical Engineering

National institute of technology, Rourkela

ABSTRACT

A non-linear converging die profile for extrusion of square section from round billet was designed using cosine function. MATLAB 7.1 was used to find out the co-ordinates of the cosine die profile. A solid model was generated using AutoCAD 2008 from the above generated points. The STL files of extrusion die generated in AutoCAD was used in DEFORM-3D for FEM simulation. Experimental investigation of extrusion of square section from round billet using non-linear converging dies were done for different percentage of reduction of cross section in dry and lubricated condition. All the experiments were done using FIE' Electronic Universal Testing machine (UTM), model UTS-100 with maximum capacity of 1000 kN with accuracy ±1.0% kN. Material properties of lead like flow stress and friction factor were determined using compression and ring compression tests under different boundary conditions. To study the flow pattern of the material during extrusion, experiments were done with split work piece in lubricated condition by making grid. The extrusion load with punch travel was compared with extrusion load with solid work piece under same experimental condition. It was found that extrusion load in splitted work piece is less than the work piece when solid. FEM simulation of extrusion of square section from round billet for pure Lead and aluminium-1100 as work material were done using DEFORM-3D 6.1 (sp1). For FEM simulation the linear converging and cosine (non-linear converging) die profiles are used. FEM simulation using leads were done for two frictional conditions 0.38 and 0.75 corresponding to dry and lubricated conditions. Extrusion was assumed to be isothermal. From present investigation it was found that the extrusion load in case of cosine (non-linear converging) die is less than the linear converging dies under same condition. The extrusion load increases with increase in reduction and friction factor.

CONTENTS

LIST OF FIGURE

LIST OF TABLES

Chapter 1

INTRODUCTION

Chapter 1

Introduction

1.1 History of Extrusion

Extrusion is an often-used forming process among the different metal forming operations and its industrial history dates back to the 18th century. In 1797, Joseph Bramah an English inventor patented the first extrusion process for making lead pipe. It involved preheating the metal and then forcing it through a die via a hand driven plunger. In the past 30 years, its economic importance has increased, primarily as a result of technological advances that have drawn on extensive practical experience and on numerous fundamental investigations into the extrusion process, tooling, and metal flow. The development of the extrusion press from the first dimple lead press to the modem automatic extrusion plant represents a chapter in the history of metalworking. Several important dates mark the path to the versatile process used today for both nonferrous metals and steel. A brief summary is given below:

In recent years, researchers started to be attracted by three-dimensional problems in metal forming. At present three-dimensional modeling is still regarded as a highlighted and difficult problem. Different methods of analysis have been extended to three dimensional, among which the finite element analysis is most commonly used. Most of the papers published on three dimensional finite element method simulations are based on different software package like ALGOR, DEFORM-3D etc.

1.2 Definition of Extrusion

Extrusion can be defined as the process of subjecting a material to compression so that it is forced to flow through a confined space past a suitable opening called the die. The metal is forced through the die and the cross-section of the die determines the shape properties of the resulting product. Extrusion may be done either on cold metal or on heated metal. One of the analogies that can be offered to the process of extrusion is that of squeezing a tube of toothpaste. The metal billet is placed in the billet chamber and is forced by the ram through a die.

Hot extrusion is done to eliminate the cold working effects, reduce the force required, and reduce directional properties. However cold extrusion is also possible for many metals and has become an important commercial process. The reaction of the billet with the container and the die results in high compressive stresses that effectively reduce cracking of materials during primary breakdown from ingot. This is an important reason for increased commercial adoption of extrusion in the working of metals difficult to form such as stainless steel, nickel, nickel based alloys and other high temperature materials. Lead, brass, bronze, copper, aluminum, and some of the magnesium alloys are the most commonly extruded metals.

In general extrusion is used to produce cylindrical bars or hollow tubes. A large variety of irregular cross sections are also produced by this process using dies of complex shapes. The process has definite advantage over rolling for production of complicated section having re-entrant corners. In this process large reduction achieved even at high strain rates has made it one of the fastest growing metal working methods.

1.3 Classification of Extrusion

According to the flow direction of metal with respect to ram movement direction extrusion process can be classified under the following methods

- Direct extrusion
- Indirect extrusion
- Impact extrusion.

1.3.1 Direct Extrusion

Direct extrusion is a process where the flow of material through the die is in the direction of the movement of the ram that is used to force the material. Here the billet is moved forward relative to the wall of the container, thereby giving rise to high resistance from friction.

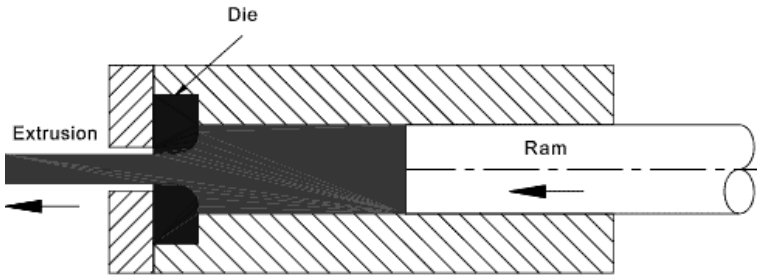

Figure 1. Direct extrusion

1.3.2 Indirect Extrusion

Indirect extrusion is a process where the flow of the material through the die is in a direction opposite to the movement of the ram that is forcing the material to deform. Here there is no relative motion between the container and the billet and, therefore, the frictional force is minimal.

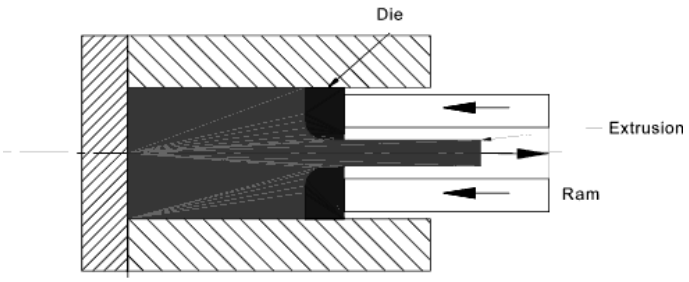

Figure 2. Indirect extrusion

1.3.3 Impact Extrusion

Impact extrusion is a process where a single blow from the ram on the material causes the metal billet to be extruded between the die and the punch. This process is usually done cold and on low strength ductile materials such as lead, tin and aluminum. It is used to make collapsible tubes for toothpaste, shaving cream, and cans that are used to pack food.

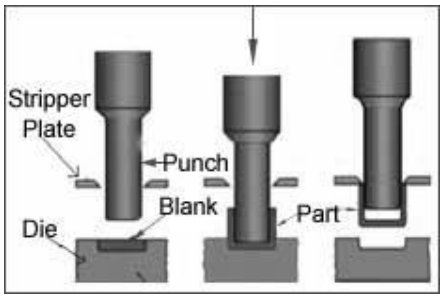

Figure 3. Impact extrusion

1.4 Die Design Consideration

For die design of extrusion following factors are to be considered as given bellow.

- Desired shape of the product
- Material
- Billet size
- Process capacity

- Extrusion ratio
- Number of die cavities
- Shrink factor
- Process tool
- Extrusion temperature
- Extrusion pressure
- Die material
- Heat treatment of die material

1.5 Equipment Used

The equipment on the basis of the type of force used to drive the ram is classified as follows:

1.5.1 Hydraulic Press

In this type of equipment the force required to derive the ram (punch) is supplied by hydraulic means to deform the metal plastically

1.5.2 Mechanical Press

In this type of equipment the force required to derive the ram (punch) is supplied by mechanical means to deform the metal plastically

1.6 Advantages of Extrusion

Among the different metal forming processes, extrusion has definite advantages over others for the production of three dimensional section shapes. Now it is becoming essential to pay greater attention to the extrusion of section rod from round stock, as this operation offers the promises of

an economic production route. The process is also attractive because press machines are readily available and the necessity to purchase expensive section stock corresponding to a multiplicity of required sections is eliminated. There are many advantage of extrusion as follows

- Uniform cross-sectional area over a long length.
- Low cost of dies making it economical to make small quantities of a shape.
- Good surface finish.
- Strain and hardness are increased due to strain hardening

1.7 Limitations of Extrusion

Every process has some limitation; extrusion has also some limitation as given bellow

- Most materials require high temperature and pressure, which makes the equipment costly.
- Die material should be able to withstand the load, high temperature, and wear.
- In the case of steel, the equipment is costlier due to the magnitude of temperature to which the metal must be heated. (2300 F).
- Indirect extrusion complicates the handling of the extruded parts.
- Extrusion is limited to only a few metals and cannot be done on any metal chosen.

1.8 Applications of Extrusion

Extrusion is one of the most important methods of metal forming process with we can produce many product of high industrial applications with good quality. Some of the applications of the extrusion process are given bellow

- Helicopter blades

- Turbine blades
- Wingspans
- Columns used for creating structures
- Construction material

1.9 Metal Forming

Metal forming is defined as the plastic deformation of a billet between tools to obtain the final configuration. It may be classified into five categories

- Mechanical working
- Casting
- Powder and fiber metal forming
- joining process

Forming is generally employed for those components, which require high strength, high resistance to shock and vibration, and uniform properties.

1.10 Metal Forming Analysis

The analysis of the stresses in the metal working process has been an important area of plasticity for the past few years. Since the forces and the deformations generally are quite complex. It is usually useful to use simplifying assumptions to obtain a traceable solution. As the strain involved in plastic deformation process is very large, it is usually possible to neglect elastic strain and consider only the plastic strain (rigid-plastic region). The strain hardening is also neglected. The principal use of analytical study of metalworking process is for determining the forces required to produce a given deformation for a certain geometry prescribed by the process

and is the ability to make an accurate prediction of the stress, strain, and velocity at every point in the deformed region of the work piece. Since the calculation are useful for selecting or designing the equipment to do a particular job. In this area an existing theory is generally adequate for the task. In general, any theory consists of three sets of equations.

- Static equilibrium of force equation
- Levy Mises equation
- Yield criterion

1.10.1 Upper Bound Solution

An upper bound analysis provides an overestimation of the required deformation force. It is more accurate because it will always result in an overestimation of the load that the press or the machine will be called upon to deliver. In this case factor of safety will be automatically built in. In this analysis, the deformation is assumed to take place by rigid body movement of triangular blocks in which all particles in a given element moves with the some velocity.

A kinematically admissible velocity should satisfy the

- Continuity equation
- Velocity boundary condition
- Volume constancy condition

The power of deformation calculated from this is higher than the actual one, called upper bound. When applying upper bound, the first step is to conceive of a velocity field for the deforming body.

- The field can be easily imagined and related to our visual experience.
- Velocity can be measured directly and is easily displayed in a physical manner.
- In this case factor of safety is automatically in built

- It is comparatively easy to analyze.

There exists an infinite no stress field that satisfy the upper bound solution.

1.10.2 Finite Element Analysis

The finite element analysis method represents an extension of matrix method for the analysis of framed structures to the analysis of the continuum structure. The basic philosophy of this method is to replace the structure i.e. the continuum having an infinite or unlimited number of unknowns by a mathematical model, which has a limited or finite number of unknowns at certain chosen discrete points. This method is extremely powerful as it helps to accurately analyze structures with complex geometrical properties and loading condition.

In finite element method, a structure or a continuum is discredited and idealized by using a mathematical model, which is an assembly or subdivision or discrete elements. These elements known as finite elements are assumed to be interconnected only at the joints called nodes. Simple functions such as polynomials are chosen in terms of unknown displacements and or their derivative at the nodes to the approximate over the variation of the actual displacements over each finite element. The external loading is also transformed into equivalent forces applied at the nodes. The behavior of each element and later as an assembly of these elements is obtained by relating their response to that of the nodes in such way that the following basic conditions are satisfied at each node.

- The equation of equilibrium.
- The compatibility of displacements.
- The material constitutive relationship.

The equation, which are obtained using above condition and then these modified equations are solved to obtain displacements at the nodes, which are the basic unknowns of the finite element method. Finite element method involves extensive computations mostly repetitive in nature. Hence, this method is suitable for computer programming and solutions. Finite element computer programs have become widely available, easier to use and can display results with attractive graphics. Even an inept user can produce some kind of answer. It is hard to disbelieve finite element results because of the effort needed to get them and the polish of this presentation. However, smooth and colorful stress contours can be produced by any model, good or bad. It is possible that most finite element analyses are so flawed that they cannot be trusted. Even a poor mesh, improper element type, incorrect loads or improper supports may produce results that appear reasonable in causal inspection.

1.11 Present Work

The objectives of the present work are as follows:

- Design of die profile for extrusion of square section from round billet using cosine function.
- FEM modelling of Extrusion of square section from round billet using the above die profile
- Experimental investigation for study of flow pattern of material in non-linear converging die
- Derivation of kinematically admissible velocity field for extrusion of square section from round billet using dual stream function for upper bound analysis

Chapter 2

LITERATURE REVIEW

Chapter 2

Literature survey

Introduction-

In this chapter we search few selected research paper related to Extrusion process using Upper -Bound Method and Finite Element Analysis Method. We classified all the paper in to two different categories, i.e. paper related upper bound method and paper related to finite element analysis.

2.1 Upper Bound Method

Sahoo et al. [1] reformulated the SERR technique so that it can be used for analyzing extrusion of round billets. The circular cross-section of the round billet is approximated by a regular polygon of equal area and the number of sides of the polygon is increased progressively until convergence of the extrusion pressure is achieved. As a test, the extrusion of hexagon-section bars from round billets through linearly converging dies is analyzed. It can also be used for other section's billets like channel section, triangular section, square section etc.

Sahoo et al. [2] presented an upper-bound analysis for the extrusion of bars of channel section from square/rectangular billets through rough square dies. A class of kinematically admissible discontinuous velocity fields, based on the reformulated SERR technique, is examined and the velocity field giving the lowest upper-bound is identified. This velocity fields is used to compute the upper-bound extrusion pressure for various area reduction

Maity et al. [3] proposed an upper-bound analysis for the extrusion of square sections from square billets through curved dies having prescribed profiles. They derived kinematically-admissible velocity fields using dual-stream-function technique. They present analytical results for both sticking friction and frictionless condition. For sticking friction condition they optimize the die geometry with respect to appropriate parameters. They found that in case of cosine die extrusion pressure is low in frictionless condition because entry and exit angle is zero. Under sticking-friction conditions the best upper-bound is provided by a straight tapered die.

Narayanasamy et al. [4] proposed streamlined extrusion dies by modifying the conventional extrusion dies to incorporate gradual reduction in the area of cross-section in order to ensure smooth flow of metal and to dispense with the problems faced by the conventional dies such as formation of dead metal zone, non-uniform flow of metal, more redundant work etc. The profile of the streamlined extrusion dies is the crucial parameter to optimize the extrusion process. Many profiles such as third order polynomial equation, fifth order polynomial equation, Bezier curve, etc., have been suggested for the design of streamlined extrusion dies with the view to reduce the extrusion load for the given reduction ratio. They suggested extrusion dies with cosine profile to extrude circular billet to circular shape and using upper bound solution plastic deformation work required for extrusion is determined. It has been proved that the die designed based on cosine profile is superior to the conventional shear dies and the straightly converging dies.

Sahoo et al. [5] reformulated spatial elementary rigid region (SERR) technique so that it can be used for analyzing extrusion of round billets. The circular cross-section of the round billet is approximated by a regular polygon of equal area and the number of sides of the polygon is increased progressively until convergence of the extrusion pressure is achieved. As a test, the

extrusion of triangular section bars from round billets through linearly converging dies is analyzed

Altan et al. [6] analyzed the deformation of the material during a 90° equal-channel angular extrusion (ECAE) process using upper-bound theorem. The model suggested includes the effect of friction between the sample and the die walls, radius of inner corner of the die and the dead metal zone on the deformation patterns during ECAE. The parameters of the model are explored in relation to the deformation of the material during the process. Further directions for progress in deformation analysis in severe plastic deformation processes are outlined.

Ajiboye et al. [7] studied the effect of die land length to the extrusion pressure. They found that extrusion pressure increases with increase in complexity of die geometry; for particular reduction and die length, the extrusion pressure is highest for rectangular section and lowest for square section. They found that for a particular reduction in area extrusion pressure increases with increasing die land length and vice-versa.

Paydara et al. [8] analyzed the equal channel angular extrusion with circular cross-sections using upper-bound analysis, and the power dissipated on all frictional and velocity discontinuity surfaces are determined and the total power optimized analytically. The theoretical results is compared with experiments, and it is found that the size of the plastic deformation zone and the relative extrusion pressure increase with increasing the constant friction factor. In addition the results show that there is a good agreement between the theoretical and experimental load displacement curve**.**

Kim et.al [9] derived the generalized velocity field for three-dimensional square-die forward extrusion of circular-shaped bars using billets of regular polygon. They determine the upper-bound extrusion load; the velocity distribution and the average length of the extruded billets by

minimizing the total power consumption with respect to chosen parameters by the proposed simple kinematically-admissible velocity field. It is found that the theoretical predictions and experimental results of the extrusion load and the average extruded length are in good agreement.

Sahoo [10] studies some experimental result of extrusion of hexagon, channel, triangle and cross sections using square dies and compare with theoretical result (using SERR technique)

Kim et al. [11] calculated the powers required in the steady-state CONFORM process. For this, similarity is applied to the CONFORM process for an equivalent side extrusion process, to which the upper bound method is used to derive the equation for calculating the powers. Even though the global flow characteristics between the real and the simplified processes are not similar, the calculated results for both processes show good agreement. And FEM simulation were carried out using the DEFORM software in order to verify the theoretical results.

Gordon et.al [12] used the adaptable die design method, in conjunction with an upper bound method that allows the rapid evaluation of a large number of die shapes and the discovery of the one that produces the desired outcome. A double optimization process is used to determine the values for the flexible variables in the velocity field and secondly to determine the die shape that best meets the given criteria.

Venkata Reddy et al. [13] presented the optimal design of axisymmetric dies using upper-bound method and finite-element method (FEM). They modeled billet material during plastic deformation process as visco-plastic rate sensitive material and flow stress to be strain rate and temperature dependent. They observed that the optimal die length decreases with friction factor and increases with reduction ratio and ram velocity. The extrusion power required is lowest for the stream-lined die with cosine die following closely behind. However hyperbolic dies are better

than the conical die at lower reduction ratios, whilst the conical die is superior at greater reduction ratios.

Sinha et al. [14] described the procedure for the design of a multi-hole extrusion process. For the same sizes of the holes, the ram force in a single-hole extrusion process is more than in a multi-hole extrusion process. Therefore, a simplified upper bound and slab method analysis has been carried out for a single-hole extrusion process. The ram and die pressures obtained from this analysis are used for designing a multi-hole extrusion process setup. The stresses in the die are computed using the finite element method. Based on this approach, an experimental setup was fabricated and experimental study was carried out.

Johnson [15] investigated the effects of section shape and punch speed on the necessary extrusion load, and the nature of the flow of metal within the extruded rod for extrusion of pure lead and tellurium lead rods of circular, square, rectangular, triangular and I section. It is shown that, for a given reduction in area, the load is independent of section shape for all but re-entrant shapes and increases with increase in extrusion speed.

Maity et al. [16] studied the effect of mathematically contoured die on surface integrity of extruded product. They used three dimensional upper bound methods using dual stream function method to obtain non-dimensional extrusion pressure and optimum die length for cosine die profile for different reductions. They found that the experimental results are compatible with the theory.

Basily and Sansome [17] calculated the maximum reduction of area obtainable for drawing section from a lower bound analysis they found that this reduction is less than when drawing round rod from round bar. They presented a lower bound solution in detail and compared the upper bound solution and found that, not only the draw stress can be calculated but the

equivalent die angle can be optimized for every relevant combination of the coefficient of friction and percentage reduction in area.

Nagpal and Altan [18] introduced the concept of dual stream functions to express three dimensional metal flows in the dies and analyzed the force of extrusion from round billet to elliptical bars.

Yang and Lee [19] proposed a new method of analysis for the extrusion of arbitrarily shaped sections through curved die profiles. They found a kinematically admissible velocity field by deriving the equation of a stream line. To determine the extrusion pressure for the rigid-perfectly plastic material upper-bound method is then applied. They obtained general formulation for an arbitrary cross section using conformal transformation. They discussed the effects of sectional shape, die profile and interfacial friction at the die surface.

Prakash and Khan [20] suggested a generalized expression for the spherical flow field generated by plastic flow of metal through a converging die of regular polygonal cross-section. They suggested that the expression is valid for all the possible boundary shapes of the zone of plastic deformation. They calculated the working stress for a rigid-perfectly plastic material by applying upper-bound techniques assuming that the boundaries of the zone of plastic deformation are exponential cylindrical surfaces. A constant frictional stress is assumed to be acting over the entire die-material interface. The working stress relation is minimized with respect to the shape of the boundaries of deformation zone, thus yielding a better upper-bound value of the working stress compared to the working stress for cylindrical boundaries. The effects of various process parameters on the working stress and the shape of the zone of deformation are given in graphical form. The analysis predicts optimum, dead zone and critical angles. Comparisons with earlier

theories have been made and it is concluded that the theory presented is a more generalized theory and yields better results for large die angles.

Gatto and Giarda [21] analyzed three-dimensional kinematic model by limit analysis for plastic deformation, denoted as SERR (Spatial Elementary Rigid Regions), in more detail. They found that the characteristics of some spatial figures, which are considered as particularly useful in partitioning the plastic volume in the limit analysis of the three-dimensional cases are given, together with some simple applications of the methods to practical cases of extrusion.

2.2 Finite Element Analysis

Halvorsen and Aukrust [22] studied the buckling or waving of extruded flat sections using Lagrangian FEM software, MSC Super Form. They performed some extrusion experiments to verify both the simulations and the mechanisms observed in the FEM simulations.

Lof and Blokhuis [23] presented a method for the simulation of the extrusion of complex profiles, which can be used in an industrial environment. They modeled bearing area with an equivalent bearing model to describe the resistance in the bearing without using a large number of elements. The developed a specialized pre-processor to avoid the time-consuming and complex work necessary for the development of the FEM model for a particular die.

Gang et al. 24] performed a 3D computer simulations to determine the effects of the ram speed and the billet temperature on the extrusion temperature and the peak extrusion pressure The ram speed and the billet temperature are the primary process variables that determine the quality of the extruded magnesium profile and the productivity of the extrusion operation. The optimization of the extrusion process concerns the interplay between these two variables in relation to the extrudate temperature and the peak extrusion pressure. The 3D computer simulations were

performed to determine the effects of the ram speed and the billet temperature on the extrudate temperature and the peak extrusion pressure, thereby providing guidelines for the process optimization and minimizing the number of trial extrusion runs needed for the process optimization. A case study on the extrusion of an AZ31 X-shaped profile was conducted. The correlations between the process variables and the response from the deformed material, extrudate temperature and peak extrusion pressure were established from the 3D FEM simulations and verified by the experiment. The research opens up a way to rational selection of the process variables for ensured quality and maximum productivity of the magnesium extrusion

Chanda et al. [25] investigated the effect of process parameter namely iso-speed and step wise ram speed on extrusion pressure the thermal response of the work piece and stress state of round bar using computer simulation. They found that step wise ram speed decrease enables the temperature to reach steady state which corresponds to nearly constant exit temperature.

Chanda et al. [26] performed the 3D FEM simulation of extrusion of aluminum to determine the state of stress, strain and the temperature of a commercial aluminum alloy going through square and round dies. They found that at the same process conditions, the state of stress in the aluminum alloy going through a round die is more favorable than going through a square die, especially at a high reduction ratio. The magnitude of the tensile stress component at the corners of the square extrudate is much higher than at the surface of the round extrudate, which makes the square extrudate more tearing prone. Simulation also reveals that while temperature evolution during the process is similar for both of the die shapes, temperature rise across the section is prominent, especially at sharp corners of the square extrudate. The magnitude of the tensile stress component at the corners of the square extrudate is much higher than at the surface of the round extrudate, which makes the square extrudate more tearing prone.

Hu et al. [27] developed a thermo-mechanically coupled elasto-plastic FEM system based on ANSYS software and the nite strain theory. They simulated the deep warm extrusion of a thin-walled cup. The basic parameters for process development and die design such as the metal flow, and the distribution of stresses, strains and temperature in the die and the workpiece, taking into account conduction, convection, radiation and plastic work, the loading-time curve, and the cause of failure on the punch, are obtained and analyzed. They found that simulation result agree with experimental results.

Bouzakis et al. [28] simulated the flow of wet ground clay ram extrusion device and by a FEM-based model, considering the von Mises criterion for the flow stress, the associative flow rule and the rigid–viscoplastic constitutive equation. The friction between clay and die is approached by the Tresca boundary condition, which proves a more realistic approach than the Coulomb friction law for the contact conditions between a plastically deforming material and a rigid surface. It is found that no sticking areas appear on the mandrel surface.

Li et al. [29] presented a results from a series of pocket designs that were modelled using finite element method (FEM) to systematically investigate the influence of the pocket design parameters on the metal flow In extrusion die design, it has become increasingly common to use ‘‘pocket’’ technology to balance the metal flow. They studied the effects of pocket angle and size on metal flow and it is shown that pocket angle plays an important role influencing metal flow velocity, whilst pocket volume has much less effect on velocity.

Peng et al. [30] used the commercial FEM code FORGE3 to study the influence of the number and the distribution of die holes on extrusion parameters. The flow pattern, pressure requirements, and temperature histories developed are established and it is clearly shown by the

FEM simulations that agreement with experimental results is obtained. They obtained metallurgical behavior (the substructure, recrystallised grain size and the fraction recrystallised) from these simulations. They compared the results with extrusion through a single-hole die

Fang et al. [31] investigate the effect of steps in the die pocket on metal flow to produce two chevron profiles with unequal thicknesses through two-hole dies, by means of 3D FEM simulation of extrusion in the transient state. They found that the pocket step could be effectively used to balance metal flow. They demonstrate the 3D FEM to be a powerful tool in optimizing die design and decreasing the number of trial extrusion runs.

Duana et al. [32] explored the complicated interactions between die design, forming parameters (i.e. ram speed, container temperature, billet temperature and extrusion ratio) and the product qualities (extrudate shape, surface condition and microstructure) by the use of finite element modelling (FEM). The various models (such as recrystallisation, damage criteria, etc.) have been integrated into the commercial codes, FORGE2 and FORGE3, through user routines. They found that the use of an expansion chamber can significantly reduce the degree of non-uniformity in terms of the extruded product shape and properties. The character of the complex material flow is also identifiable, which is very useful to help improve die design.

Lee et al. [33] studied the effect of bearing lengths for the control of material flow in the die in hot extrusion. They used the three-dimensional non-steady analysis using the thermo-rigid–viscoplastic element method that includes an automatic remeshing module. It was found that the design equation determined bearing lengths that resulted in a fairly uniform exit velocity distribution throughout the extruded section. From the results of this study, it was found that the proposed design equation can be effectively used to estimate appropriate bearing lengths.

Chapter 3

EXPERIMENTAL WORK

Chapter 3

Experimental Work

Introduction

In this chapter we are going to discuss about the experimental work which is consist of determination of material properties for lead like flow stress, friction factor etc and experimental investigation for study of flow pattern of material using curve die.FEM simulation of extrusion of square section from round billet with cosine and taper die are also discussed in this section.

3.1 Experimental Investigation

The whole experimental investigation were done using 'FIE' Electronic Universal Testing machine (UTM), model UTS-100 which can be used for conduction test in tension, compression and transverse test of metals and other material. Maximum capacity of the machine is of 1000 kN with measuring range between 0 to 1000 kN. The accuracy of measurement of the machine is ±1.0% kN Because load required for extrusion is of compressive type so, experiments were conducted using compression test.

3.1.1 'FIE' Electronic Universal Testing machine (UTM)

The UTM consists of three major parts

- Machine frame or Loading unit
- Hydraulic system

- Electronic control panel

3.1.1.1 Machine frame or Loading unit

Machine frame and loading unit consist of two cross heads and one lower table. Center cross head are adjustable by means of geared motor. Compression test is carried out between center and lower table while tension test is carried out between center table and upper cross head. Load is sensed by means of precision pressure transducer of strain gauge type. Loading unit is shown in Fig 3.1.

Figure 4. Machine frame

3.1.1.2 Hydraulic System unit

Hydraulic system unit consists of motor pump unit with cylinder and piston. Safety valve is provided for additional safety. The hydraulic system unit as shown in Fig

Figure 5. Hydraulic system unit

3.1.1.3 Electronic control unit

Electronic control unit control the process by controlling the input parameter like load rate, strain rate, maximum load etc.

3.1.2 Selection of the work-piece

The selection of material depends upon the properties of die material and load required for deformation. Because load required for extrusion is very high so we had to select softer materials, so we select lead as workpiece material of experimental investigation. Lead is a highly dense, corrosion resistive and very soft ductile material. Properties of lead in detail are given in table 3.1 .The thermal properties of lead are as shown.

Table 1. Mechanical properties of lead

Mechanical properties		condition
Density	11300 kg/m^3	298.15 K
Young's Modulus of Elasticity	16000MPa	

Poisson Ratio	0.44	
Thermal Expansion Coefficient	29e-6	298.15 K

Table 2. Thermal Properties

Thermal Properties		condition
Melting point	600.61 K	
Boiling point	2022.15 K	
Critical temperature	5500 K	
Heat capacity	130 J/kg-K	298.15 K
Thermal conductivity	35.3 W/m-K	300 K

3.1.3 Determination of material properties

In the present investigation pure Lead (99% pure) is used as work material. Different properties of lead material like flow stress, friction factor etc are determined using different compression method. These properties are used in FEM simulation using DEFORM-3D. In compression test, a large amount of deformation can be achieved before fracture.

3.1.3.1 Compression test

This is the simplest compression tests in which a cylinder compressed axially between smooth platens. This gives the same yield stress at a tensile test with small strains when plates are well lubricated. Frictional coefficient at the die face increases as the strain increase a specimen spreads out. From compression test we flow stress of the material can be determined. A lead solid cylinder with 30mm diameter and 50mm length is compressed between well lubricated

smooth plates as well as in dry condition to determined friction coefficient in lubricated and dry condition both. Due to flow of material diameter increases as length decreases. By turning operation extra material removed to get initial diameter.Test is repeated three times and average true stress vs. true strain graph is plotted

3.1.3.1.1 Experimental Procedure

Pure lead cylinders with a 50mm × 30 mm (H× D) were taken to obtain the stress-strain curve by a compression test using 'FIE' Electronic Universal Testing machine (UTM), model UTS-100 at room temperature. The compression rate is maintained same as that adapted for the experiments. The specimen has oil grooves on both the ends to entrap lubricant during the compression test. The compression load is recorded at every 0.5 mm of punch ravel. After compressing the specimen to about 10 mm it is taken out of the press. Compressed material re-machined to cylindrical shape with original diameter, and tested in compression till the specimen is reduced to another 10 mm. The stress-strain diagram was drawn. The average flow stress of the pure lead is found to be 48.85 N/mm^2

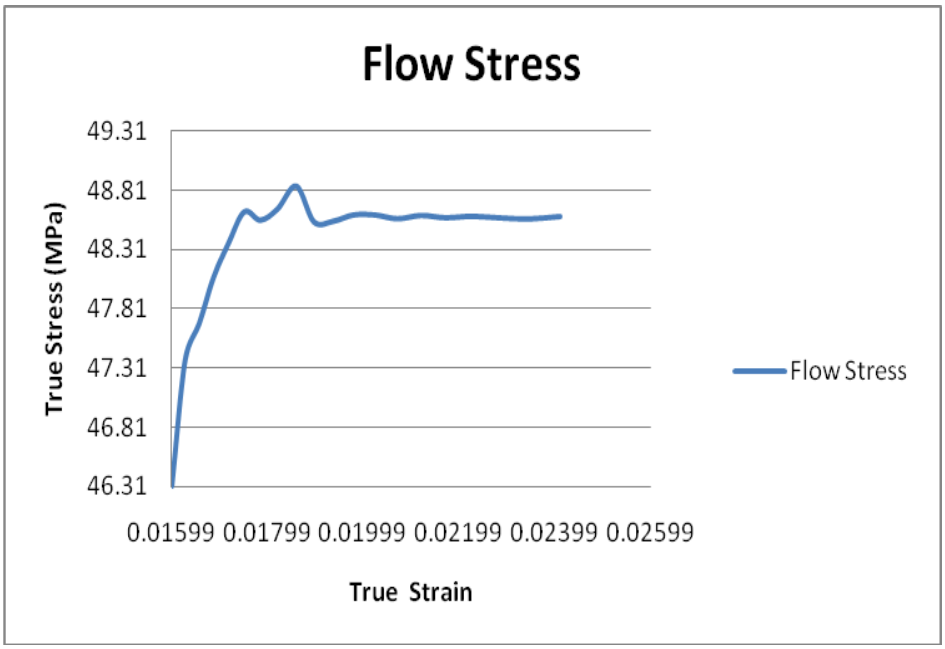

Figure 6. Flow stress

3.1.3.2 Measurement of Friction Factor

The local value of the friction cannot be easily determined. The coefficient of friction may actually vary through a working pass, as the lubrication deteriorates due to thinning of the film and extension of their surface. Experimental studies suggests, however that this is negligible for all well lubricated operations. There is at present no generally accepted method of measuring the value of the coefficient of friction for given surface and lubricant. Various factors can influence the result, chemical condition, lubricant film thickness, temperature, speed, environment and degree of deformation should match as closely as possible the actual conditions of the operation. The friction factor can be measured by the following methods.

- Direct measurement of friction in metal working
- Coefficients obtained from correlation of theory
- Measurements depending upon shape change.

3.1.3.2.1 Ring Compression Test

If the coefficient of friction can be deduced from a change in shape, the yield stress will not enter the derivation, provided the material is homogeneous and there are no serious temperature gradients. Such methods are generally suitable for rapidly strain hardening materials. Ring compression test suggested by Kudo and Kungio and developed by Cockcroft utilizes axial compression of a ring between flat platens. When a flat, ring shaped specimen is upset in the axial direction, the resulting shape change depends only on the amount of compression in the thickness direction and the frictional conditions at the die ring interfaces. If the interfacial friction were zero, the ring would deform in the same manner as a solid disk, with each element flowing outward radial from the center.

In case of small but finite interfacial friction, the outside diameter is smaller than in the zero friction case. If the friction exceeds a critical value, frictional resistance to outward flow becomes so high that some of the ring material flows inward to the center. Measurements of the inside diameters of compressed rings provide a particularly sensitive means of studying interfacial friction, because the inside diameter increases if the friction is low and decreases if the friction is higher. The ring thickness is usually expressed in relation to the inside and outside diameters. Under the condition of maximum friction, the largest usable specimen height is obtained with rings of dimensions in the ratio of 6:3:1 i.e. outer diameter: inner diameter: height. For normal lubricated conditions, geometry of 6:3:2 can be used to obtain results of sufficient accuracy for most applications. The ring compression test can be used to measure the flow stress under high strain practical forming conditions. Thus, by measuring the ratio of internal, external diameters after axial compression of a ring of standard dimensions, it is possible to obtain a measure of the friction.

3.1.3.2.1.1 Experimental Procedure for ring test

A ring compression test was carried out at dry condition and commercially available grease lubrication condition. The rings were compressed up to the 4 mm inner diameter, at each 0.5 mm Of punch travel inner diameter and height was recorded. The friction factors were found to be 0.75 for dry condition and 0.38 for the lubricated condition by comparing our result with the calibration curve of Male and Cockcroft as shown in the fig. 3.3

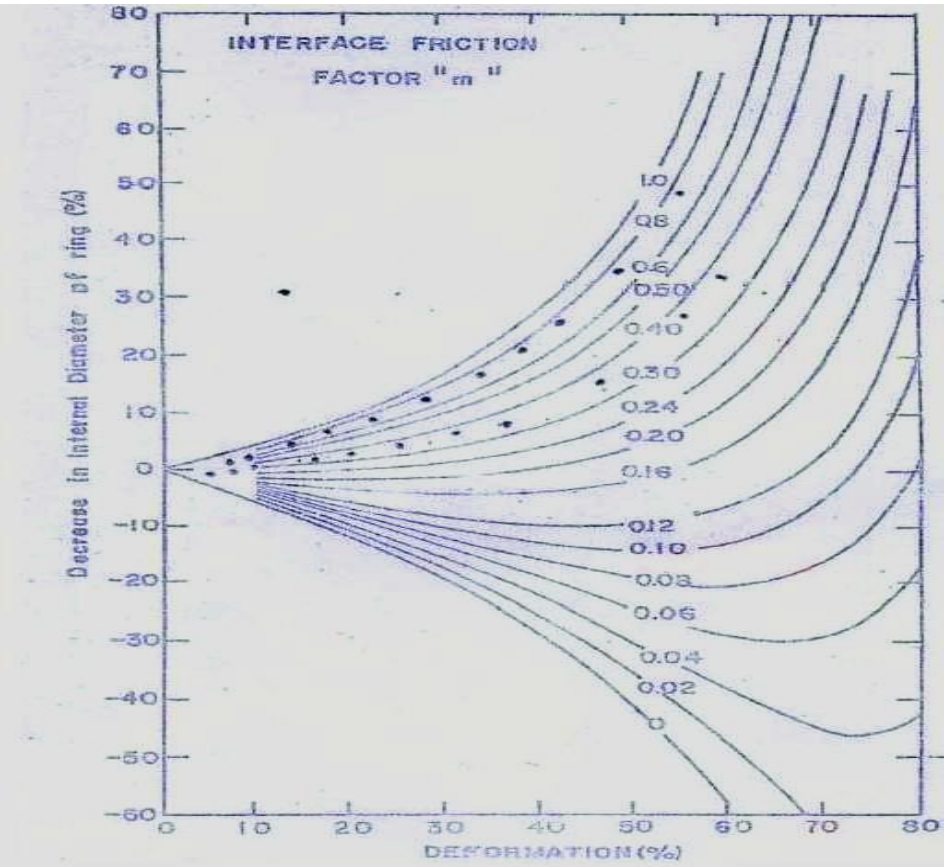

Figure 7. Theoretical calibration curve for standard ring 6:3:2

3.1.4 Different Parts of the Set-up

Main part of the setup consist of the following parts

- Die holder
- Container or Extrusion chamber
- Punch and supporting plate
- Die plate

Figure 8. Different parts of die set

All the setup parts are made up of Mild steel with tensile strength - 320 N/mm^2 and Hardness 100 BHN

Dies are manufactured split type for easy removal of the product. For present experimental investigation of extrusion of square section from round billet split type of dies of three reductions 50%, 70% and 90% are used.

3.1.5 Experimental procedure

Before starting the test the die sets, die holder and inside face of extrusion chamber were cleaned. The two halves of the die set were then push fitted into die holder and total assembly were secured by screwing four bolts. The full assembly was then placed in between the base plate and center table of 'FIE' Electronic Universal Testing machine (UTM), model UTS-100 in upside down position. It was done so that extrude product would get enough clearance, when it comes out from the die. For carrying out an extrusion test the pure lead specimen was placed inside the extrusion chamber or container. The punch was then inserted into its position. After centering the apparatus under machine lower table, Machine was started and extrusion process was continued. Punch load was recorded at every 1 mm movement of punch travel, which was read from computer fitted to the UTM. The application of load was continued till it reaches the steady state and up to certain length of product comes out side. At this position Machine was stopped and test was terminated the die holder was then separated from extrusion chamber and finally die halves with extruded product were pushed out from die holder and extrusion chamber. Experiments were conducted for three different reductions 50%, 70% and 90% to get square section product at two different experimental conditions (dry and lubricated) from round cross-section billet.

Figure 9. Extruded material with different reduction

3.1.6 Split Test

To study the flow pattern of the material during extrusion of square section from round billet using non-linear converging dies for different reduction, split test was done.

3.1.6.1 Procedure of Split Test

Lead material round billet of 30mm diameter and 50mm length is taken as work material, the work material is spited in to two parts along it diameter. A grid of 5mm x 5mm is made in to inner surface of the slitted part. In fig 5 grid pattern is shown. Rubber band is put in to the grid pattern to prevent material mixing during extrusion, because lead is a very soft ductile metal. Now, both part are again join using araldite (gum) and clamp it for 48 hour so that both part joined properly like single piece.

Figure 10.Splited work material with grid before extrusion

Extrusion is carried out in lubricated condition of split work material. The flow pattern is studied for different percentage of reduction. Work material after extrusion with 50% reduction is shown in fig 6. In fig 7 flow pattern of material with 70% reduction in area is shown. Fig 8 shows the flow pattern of material with 90% reduction

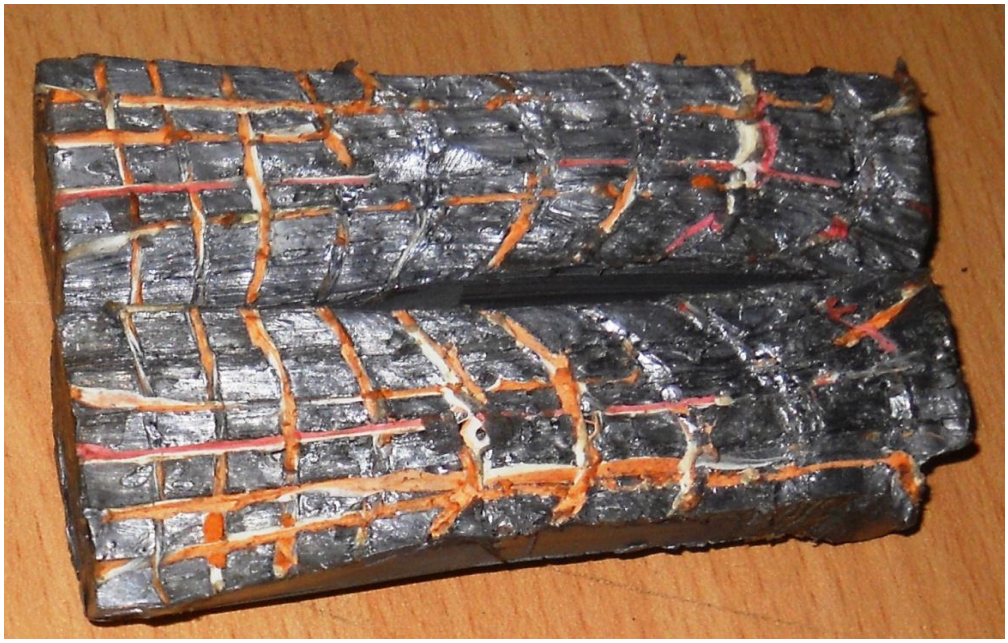

Figure 11. Flow pattern of material with 50% reduction

Figure 12. Flow pattern of material with 70% reduction

Figure 13.Flow pattern of material with 90% reduction

3.2 Finite element analysis

Finite element analysis modeling is done using DEFORM-3D Version 6.1(sp1). DEFORM-3D is a Finite Element Method (FEM) based process simulation system designed to analyze various forming and heat treatment processes. By simulating manufacturing processes on a computer, this advanced tool allows designers and engineers to:

- Reduce the need for costly shop floor trials and redesign of tooling and processes
- Improve tool and die design to reduce production and material costs
- Shorten lead time in bringing a new product to market

Unlike general purpose FEM codes, DEFORM is tailored for deformation modelling. A user friendly graphical user interface provides easy data preparation and analysis so engineers can focus on forming, not on learning a cumbersome computer system.

The DEFORM-3D consists of three major components:

- Pre-processor: used for creating assembly or modifying the data required to analyze the simulation, generating mesh and for generating the required database file.
- Simulation engine: Used for performing the numerical calculations required to analyze the process, and writing the results to the database file. The simulation engine reads the database file, performs the actual solution calculation, and appends the appropriate solution data to the database file.
- Post-processor: Used for reading the database file from the simulation engine and displaying the results graphically and for extracting numerical data.

3.2.1 Simulation procedure

FEM simulation is carried out using DEFORM-3D Version 6.1(sp1). As discussed above DEFORM-3D consist of three main components. We stared with pre-processor in which we define the object of 30mm diameter and 50mm length. We generate the mesh of 10, 0000 element. We define other part of setup like Punch and container. The geometry of the extrusion die is imported in the form of STL file generated in AutoCAD. A material data is created using pure lead properties. After setting the whole setup a database (.DB) is generated.

The simulation engine reads the database file generated in pre-processor and performs the actual solution calculations, and writes the result in database file.

In post-processor, we read all the results, draw graphs, take picture of the workpiece at different steps and at different properties like stain, strain rate, velocity, displacement etc.

3.2.1.1 FEM simulation of Alluminium-1100 and pure lead

FEM Simulation using aluminum-1100 as work material was done with non-linear converging die (cosine die) and linear converging die and FEM simulation using lead was done cosine die for two frictional conditions 0.38 and 0.75 as derived from experiment using ring compression test. Simulation was done according to the simulation procedures described in previous section. It is found that the extrusion load is less in case of cosine die.

Chapter 4

DIE PROFILE DESIGN

Chapter 4

Die Profile Design

Introduction-

In this chapter we derive an extrusion die profile foe square section from round billet using cosine function. First of all a mathematical equation of the die profile is derived. Then using MATLAB 7.0.1 we calculate the co-ordinate of the die profile. The generated co-ordinates were used in AutoCAD 2008 to generate solid model of the die profile.

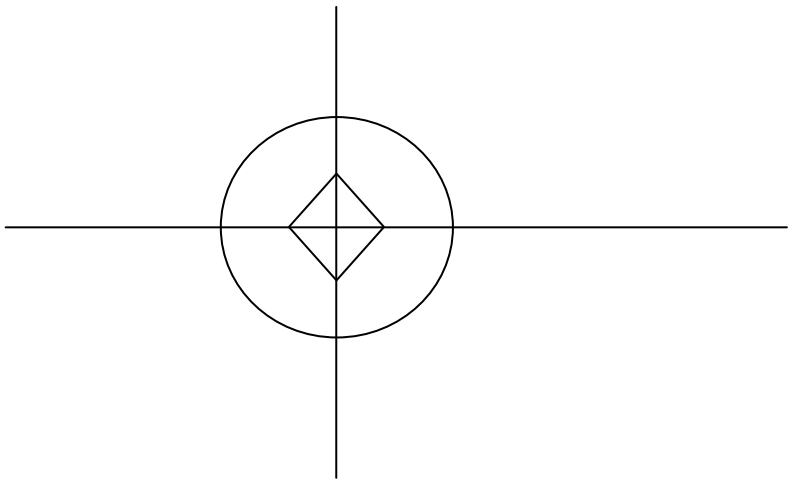

Figure 14.Cross-sectional view of the die profile

Let, R=radius of the billet.

$(\sqrt{2})A$ = length of the side of the square.

N= max. no. of steps in steps in the transverse direction for particular value of Z.

P=any step between 0 and N in the transverse direction for particular value of Z.

L=length of the die

X, Y & Z are the co–ordinate axes in three mutually perpendicular directions

Let us consider the cross-sectional view of the extrusion de which extrudes the round billet to square as shown in the above figure-14.

Taking section of die in first quadrant, we find that circular cross section changing to linear according to cosine function in longitudinal directional n no. of steps.

At the entrance the die profile is circular as shown in the above fig. 14 with equation

$x^2+y^2=R^2$ ----------(1)

Where R=radius of the circular billet at entrance of the die.

And x&y are the co-ordinate axes.

Because, cross-section f the die is changing continuously from round to square according to the cosine function, so any cross-section between the entrance and exit will be different from circular and linear.

So, at the exit of the die, profile will be linear as shown in the fig. 14 with equation

$x+y = A$ ---------- (2)

Where A= intersection of edge of the die exit on x & y axes.

And x&y are the co- ordinate axes.

Now, after (p) steps (p<N) co-ordinate of any point on circular cross-section will be

$T(x,y) =[R*\sqrt{(1-P/N)}, R*P/N]$

Similarly, after (p) steps (p<N) co-ordinate of any point on linear cross-section will be

T(x,y) =[A*(1-P/N), A*P/N]

So, general equation of any point on the cross-section using cosine function will be

$$x = \left[\frac{R*\sqrt{(1-\frac{P}{N})}+A\left(1-\frac{P}{N}\right)}{2}\right] + \left[\frac{R*\sqrt{(1-\frac{P}{N})}-A\left(1-\frac{P}{N}\right)}{2}\right]\cos\left(\frac{\pi z}{L}\right) \quad -(3)$$

And

$$y = \left[\frac{R*\sqrt{(P/N)}+A\left(\frac{P}{N}\right)}{2}\right] + \left[\frac{R*\sqrt{(\frac{P}{N})}-A\left(\frac{P}{N}\right)}{2}\right]\cos\left(\frac{\pi z}{L}\right) \quad ---(4)$$

Where P = 0, 1, 2, 3, 4… N

Hence, According to the equation (3) & (4), for every value of Z (0<Z<L) we will get N no. of value of X&Y

Now percentage fraction of reduction (1-Q)

$$\frac{\pi R^2 - 2A^2}{\pi R^2} = 1 - Q$$

$$Q = \frac{2A^2}{\pi R^2}$$

$$A = R\sqrt{(\frac{\pi Q}{2})} \quad \text{---------- (5)}$$

Case -1:

At Z=0

From equation (3) & (4) we will get N no of values of X&Y

X= $R * \sqrt{(1 - \frac{P}{N})}$

Y= $A\left(1 - \frac{P}{N}\right)$

And cross-section will be circular which is shown in the fig. 15.

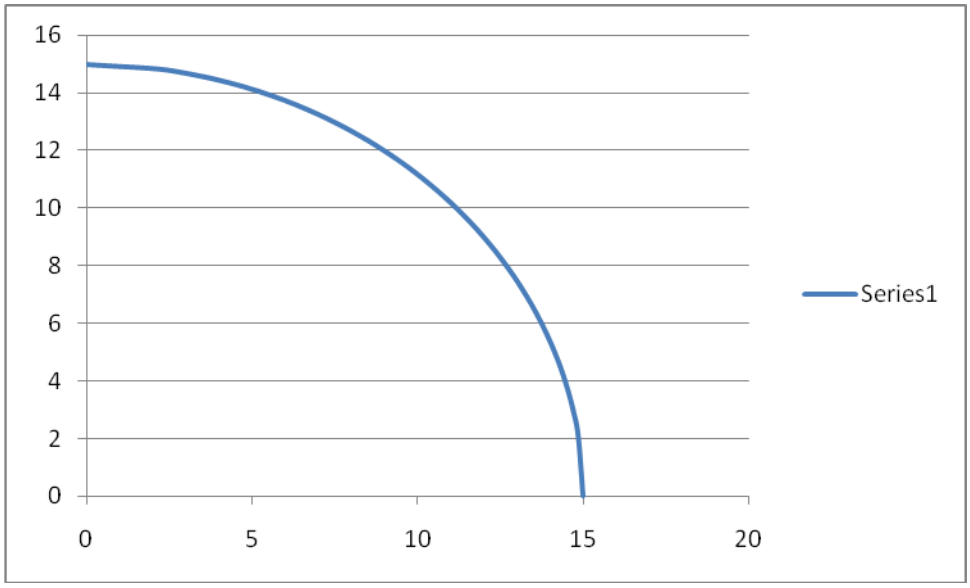

Figure 15.Cross-sectional of die profile at entrance in one quadrant

Case-2 (At Z=L)

From equation (3) & (4) we will get N no of values of X&Y

X= $R * \sqrt{(P/N)}$

Y= $A\left(\frac{P}{N}\right)$

And cross-section will be linear which is shown in the fig. 16.

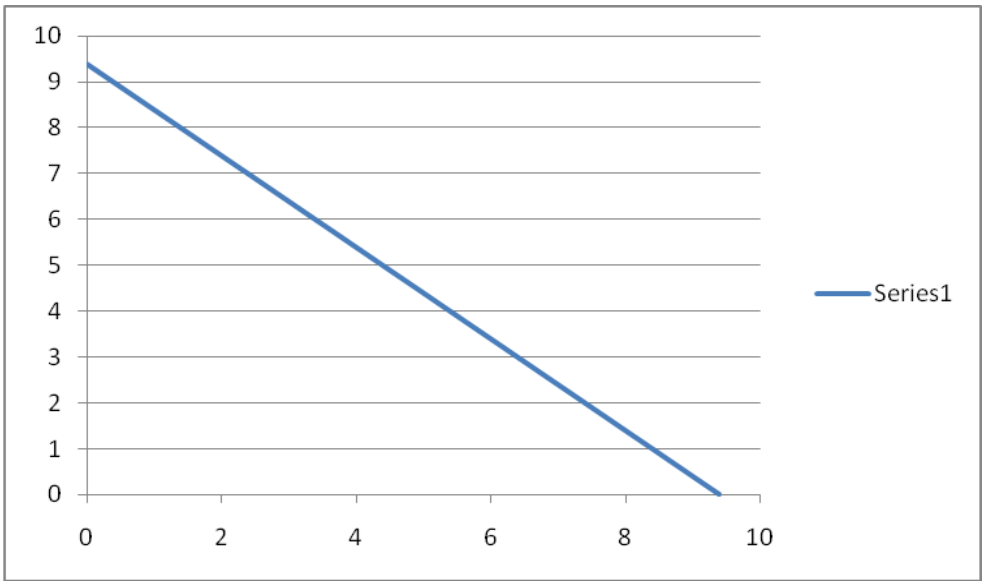

Figure 16.Cross-sectional of die profile at exit in one quadrant

At Z=L/2

From equation (3) & (4) we will get N no of values of X&Y

$$x = \left[\frac{R*\sqrt{(1)-\frac{P}{N}}+A\left(1-\frac{P}{N}\right)}{2}\right] + \left[\frac{R*\sqrt{(1)-\frac{P}{N}}-A\left(1-\frac{P}{N}\right)}{2}\right]\cos\left(\frac{2\pi z}{L}\right) \quad ---(3)$$

And

$$y = \left[\frac{R*\sqrt{(P/N)}+A\left(\frac{P}{N}\right)}{2}\right] + \left[\frac{R*\sqrt{(\frac{P}{N})}-A\left(\frac{P}{N}\right)}{2}\right]\cos\left(\frac{2\pi z}{L}\right) \quad ---(4)$$

And cross-section will be in between circular & linear which is shown in the fig. 17.

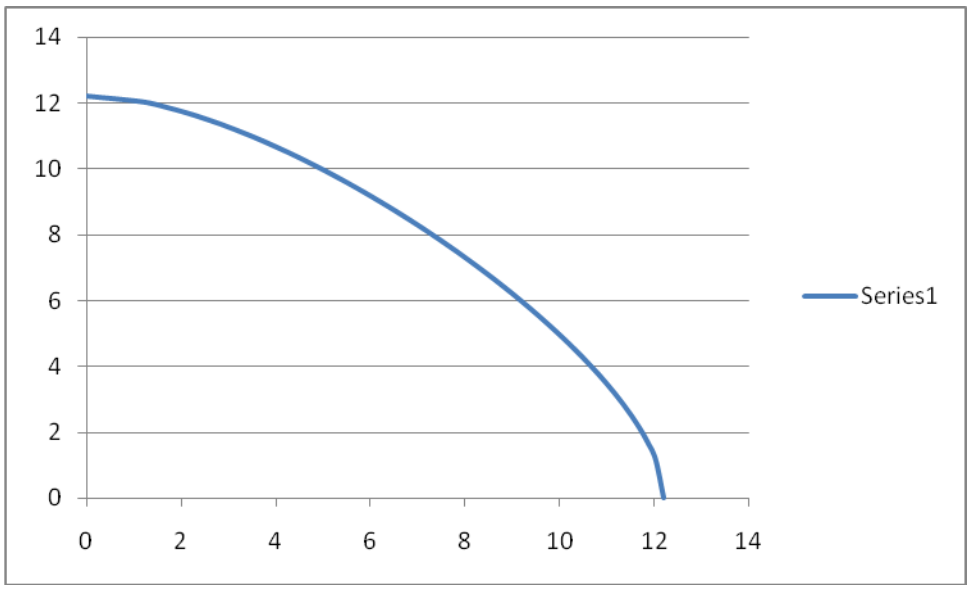

Figure 17.Cross-sectional of die profile at mid point in one quadrant

4.1 Solid Modelling

MATLAB 7.1 was used to generate the no fo points using above generated die profile equation. The generated points were used to create solid model using AutoCAD 2008. Solid model generated from AutoCAD 2008 were shon in the followin figures.

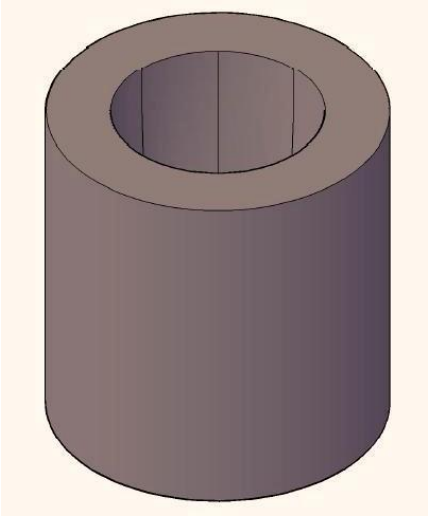

Figure 18.Solid model

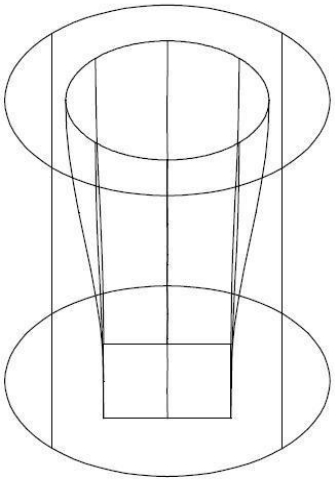

Figure 19.wire-frame model

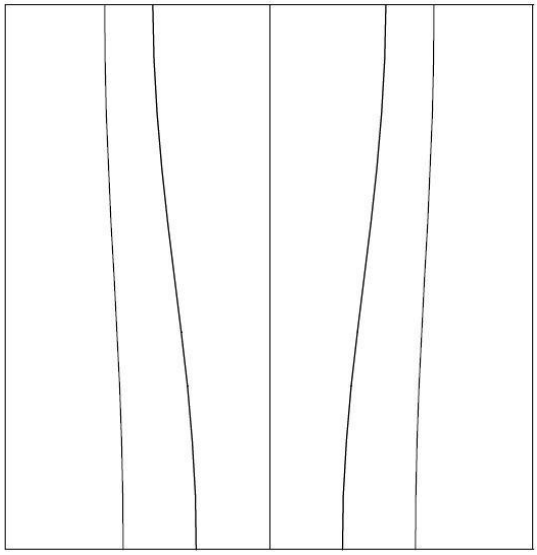

Figure 20.wire-frame longitudinal view

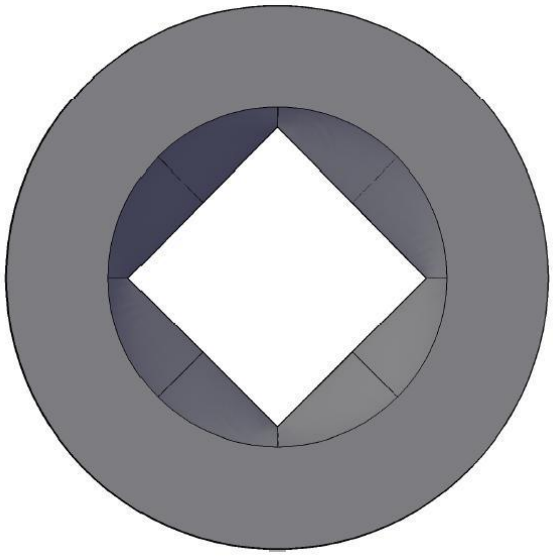

Figure 21.Top view

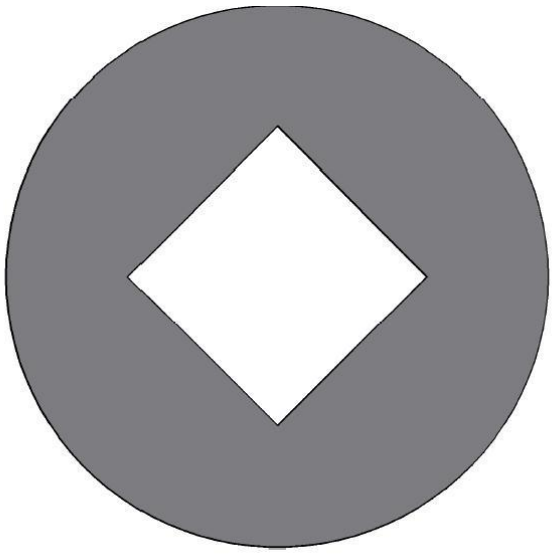

Figure 22.Bottom view

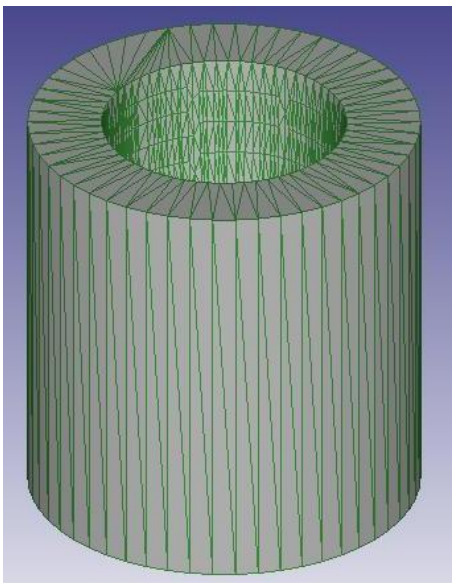

Figure 23.STL file

Fig 23 shows the STL file generated from AutoCAD 2008.

Chapter 5

DERIVATION OF KINEMATICALLY ADMISIBLE VELOCITY FIELD USING DUAL STREAM FUNCTION

Chapter 5

Derivation of Kinematicaly Admisible Velocity Field using Dual Stream Function

Introduction

In this chapter we derive a kinematically admissible velocity field using dual stream function. Cosine die profile equation which is derive in previous chapter is used as governing equation for deriving kinematically admissible velocity field using dual stream function

5.1 Dual stream function

General equation of any point on the cross-section using cosine function will be given by the equation (1) and (2)

$$F(z_1) = x = \left[\frac{R*\sqrt{(1-\frac{P}{N})}+A\left(1-\frac{P}{N}\right)}{2}\right] + \left[\frac{R*\sqrt{(1-\frac{P}{N})}-A\left(1-\frac{P}{N}\right)}{2}\right]\cos\left(\frac{\pi z}{L}\right) \quad (1)$$

$$F(z_2) = y = \left[\frac{R*\sqrt{(P/N)}+A\left(\frac{P}{N}\right)}{2}\right] + \left[\frac{R*\sqrt{(\frac{P}{N})}-A\left(\frac{P}{N}\right)}{2}\right]\cos\left(\frac{\pi z}{L}\right) \quad (2)$$

Let the stream function are

$$\varphi 1 = \frac{-x}{F(z_1)} \qquad (3)$$

$$\varphi 1 = \frac{\pi R^2 v_b y}{F(z_2)} \qquad (4)$$

Now v_x, v_y, v_z are velocity function in x, y & z direction respectively. Then velocity field in x, y and Z direction can be given as follows.

$$v_x = \left\{\frac{\partial \varphi_2}{\partial y} * \frac{\partial \varphi_1}{\partial z}\right\} - \left\{\frac{\partial \varphi_1}{\partial y} * \frac{\partial \varphi_2}{\partial z}\right\} \qquad (5)$$

$$v_y = \left\{\frac{\partial \varphi_2}{\partial z} * \frac{\partial \varphi_1}{\partial x}\right\} - \left\{\frac{\partial \varphi_1}{\partial z} * \frac{\partial \varphi_2}{\partial x}\right\} \qquad (6)$$

$$v_z = \left\{\frac{\partial \varphi_2}{\partial x} * \frac{\partial \varphi_1}{\partial y}\right\} - \left\{\frac{\partial \varphi_1}{\partial x} * \frac{\partial \varphi_2}{\partial y}\right\} \qquad (7)$$

5.2 Derivation of kinematically admissible velocity field

Using equation (1) & (2) velocity function can be written as follow

$$v_x = \left\{\frac{\partial \varphi_2}{\partial y} * \frac{\partial \varphi_1}{\partial z}\right\} - \left\{\frac{\partial \varphi_1}{\partial y} * \frac{\partial \varphi_2}{\partial z}\right\}$$

$$v_x = \frac{\pi R^2 v_b y}{F(z_2)} * \frac{x}{F(z_1)^2} \qquad (8)$$

$$v_y = \left\{\frac{\partial \varphi_2}{\partial z} * \frac{\partial \varphi_1}{\partial x}\right\} - \left\{\frac{\partial \varphi_1}{\partial z} * \frac{\partial \varphi_2}{\partial x}\right\}$$

$$v_y = \frac{\pi R^2 v_b y}{F(z_2)^2} * \frac{1}{F(z_1)} \qquad (9)$$

$$v_z = \left\{\frac{\partial \varphi_2}{\partial x} * \frac{\partial \varphi_1}{\partial y}\right\} - \left\{\frac{\partial \varphi_1}{\partial x} * \frac{\partial \varphi_2}{\partial y}\right\}$$

$$v_y = \frac{\pi R^2 v_b}{F(z_2)} * \frac{1}{F(z_1)} \qquad (10)$$

5.3 Derivation of strain function

Now $\varepsilon_{xx}, \varepsilon_{yy}, \varepsilon_{zz}$ strain function in x, y & z direction respectively

$$\varepsilon_{xx} = \frac{\partial v_x}{\partial x} \qquad (11)$$

$$\varepsilon_{yy} = \frac{\partial v_y}{\partial y} \qquad (12)$$

$$\varepsilon_{zz} = \frac{\partial v_z}{\partial z} \qquad (13)$$

Using equation (1) & (2) strain function can be written as follow

$$\varepsilon_{xx} = \frac{\partial v_x}{\partial x}$$

$$\varepsilon_{xx} = \frac{\pi R^2 v_b}{F(z_2)} * \frac{1}{F(z_1)^2} \qquad (14)$$

$$\varepsilon_{xx} = \frac{\pi R^2 v_b}{\left[\frac{R * \sqrt{(P/N)} + A\left(\frac{P}{N}\right)}{2}\right] + \left[\frac{R * \sqrt{\left(\frac{P}{N}\right)} - A\left(\frac{P}{N}\right)}{2}\right] cos\left(\frac{\pi z}{L}\right) * \left\{\left[\frac{R * \sqrt{(1 - \frac{P}{N})} + A\left(1 - \frac{P}{N}\right)}{2}\right] + \left[\frac{R * \sqrt{(1 - \frac{P}{N})} - A\left(1 - \frac{P}{N}\right)}{2}\right] cos\left(\frac{\pi z}{L}\right)\right\}^2}$$

$$\varepsilon_{yy} = \frac{\partial v_y}{\partial y}$$

$$\varepsilon_{yy} = \frac{\pi R^2 v_b}{F(z_2)} * \frac{1}{F(z_1)} \qquad (15)$$

$$\varepsilon_{yy} = \frac{\pi R^2 v_b}{\left[\frac{R*\sqrt{(P/N)} + A\left(\frac{P}{N}\right)}{2}\right] + \left[\frac{R*\sqrt{\left(\frac{P}{N}\right)} - A\left(\frac{P}{N}\right)}{2}\right] cos\left(\frac{\pi z}{L}\right) * \left\{\left[\frac{R*\sqrt{(1-\frac{P}{N})} + A\left(1-\frac{P}{N}\right)}{2}\right] + \left[\frac{R*\sqrt{(1-\frac{P}{N})} - A\left(1-\frac{P}{N}\right)}{2}\right] cos\left(\frac{\pi z}{L}\right)\right\}}$$

$$\varepsilon_{zz} = \frac{\partial v_z}{\partial z}$$

$$\varepsilon_{zz} = -\pi R^2 v_b \left\{\frac{1}{F(z_1) * F(z_2)^2} + \frac{1}{F(z_2) * F(z_1)^2}\right\} \qquad (16)$$

$$\varepsilon_{zz} = -\pi R^2 v_b \left\{\frac{1}{\left\{\left[\frac{R*\sqrt{(P/N)} + A\left(\frac{P}{N}\right)}{2}\right] + \left[\frac{R*\sqrt{\left(\frac{P}{N}\right)} - A\left(\frac{P}{N}\right)}{2}\right] cos\left(\frac{\pi z}{L}\right)\right\}^2 * \left\{\left[\frac{R*\sqrt{(1-\frac{P}{N})} + A\left(1-\frac{P}{N}\right)}{2}\right] + \left[\frac{R*\sqrt{(1-\frac{P}{N})} - A\left(1-\frac{P}{N}\right)}{2}\right] cos\left(\frac{\pi z}{L}\right)\right\}} + \frac{1}{\left[\frac{R*\sqrt{(P/N)} + A\left(\frac{P}{N}\right)}{2}\right] + \left[\frac{R*\sqrt{\left(\frac{P}{N}\right)} - A\left(\frac{P}{N}\right)}{2}\right] cos\left(\frac{\pi z}{L}\right) * \left\{\left[\frac{R*\sqrt{(1-\frac{P}{N})} + A\left(1-\frac{P}{N}\right)}{2}\right] + \left[\frac{R*\sqrt{(1-\frac{P}{N})} - A\left(1-\frac{P}{N}\right)}{2}\right] cos\left(\frac{\pi z}{L}\right)\right\}^2}\right\}$$

Adding equation (1), (2) & (3) we get

$$\varepsilon_{xx} + \varepsilon_{yy} + \varepsilon_{zz} = 0$$

Chapter 6

RESULTS AND DISCUSSION

Chapter 6

Results and discussion

Introduction

In this chapter all the results of Experimental investigation, FEM analysis are discussed. Results in different experimental conditions are compared. The results of FEM analysis are also compared with the experimental values

6.1 Experimental Investigation

The variation of compressive extrusion load with respect to punch movement was determined from the extrusion test of square section from round billet using linear converging die and non-linear converging dies. In the present investigation it is found that, the extrusion load with respect to punch travel, increase with increase in percentage reduction of cross-section.

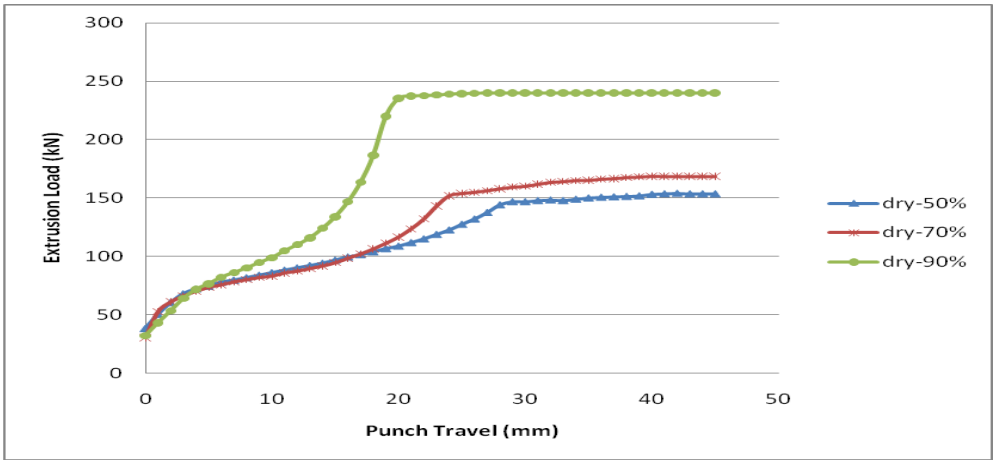

Figure 24.Comparesion of extrusion load with punch travel in dry condition for different reduction

The variation of extrusion load with respect to the punch travel in dry condition is shown in the fig.24, from fig it is clear that the extrusion load increases with increase in percentage reduction. It is also clear that initially, the load is almost same for all reduction.

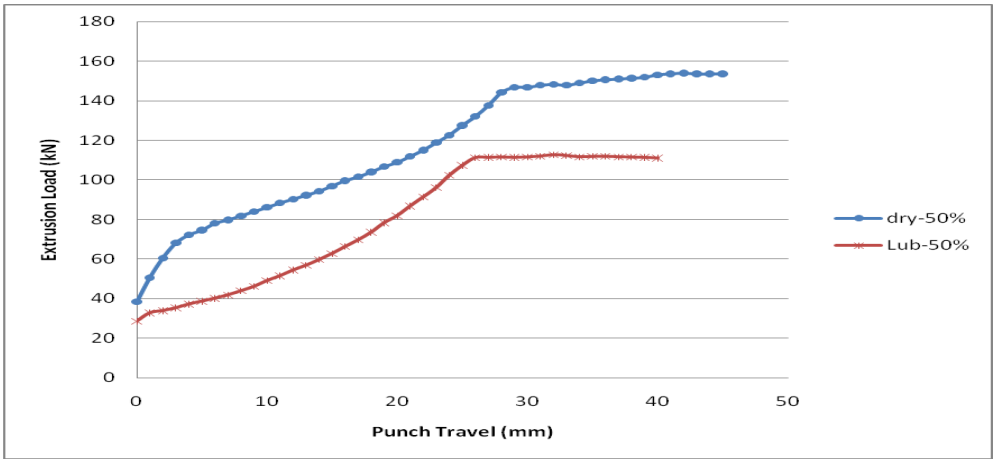

Figure 25.Comparesion of extrusion load with punch travel in dry and lubricated condition for 50% reduction

The Comparison of variation of extrusion load with respect to the punch travel in dry and lubricated condition is shown in the fig.25. It is found that the load in case of lubricated condition is less than the dry condition for 50% reduction.

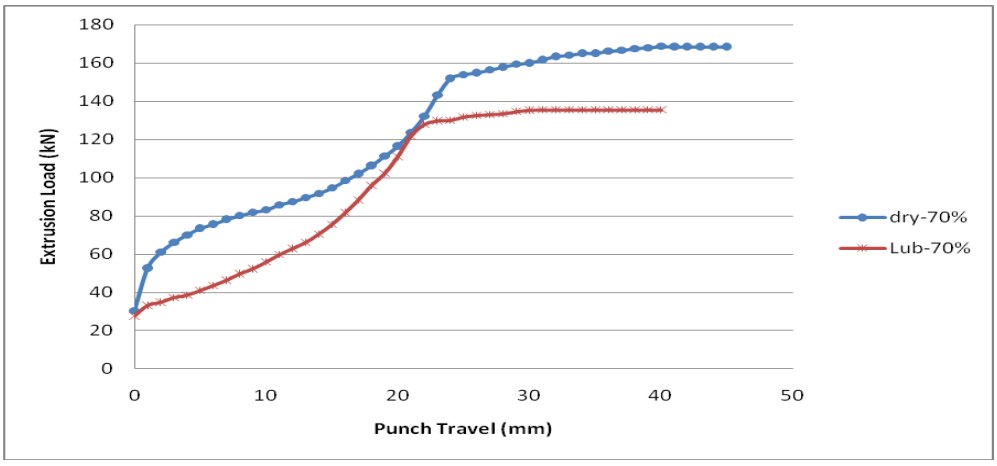

Figure 26.Comparesion of extrusion load with punch travel in dry and lubricated condition for 70% reduction

The Comparison of variation of extrusion load with respect to the punch travel in dry and lubricated condition is shown in the fig.26. It is found that the load in case of lubricated condition is less than the dry condition for 70% reduction

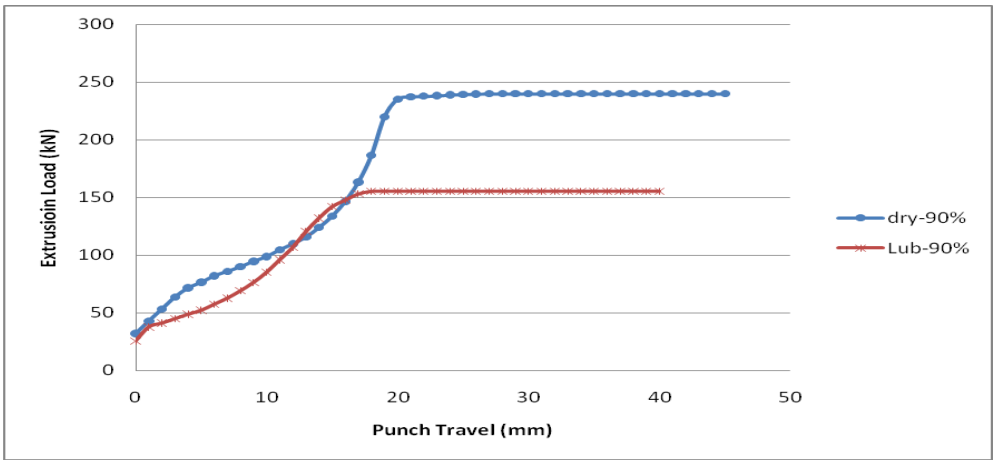

Figure 27. Comparesion of extrusion load with punch travel in dry and lubricated condition for 90% reduction

The Comparison of variation of extrusion load with respect to the punch travel in dry and lubricated condition is shown in the fig.27. It is found that the load in case of lubricated condition is less than the dry condition for 90% reduction

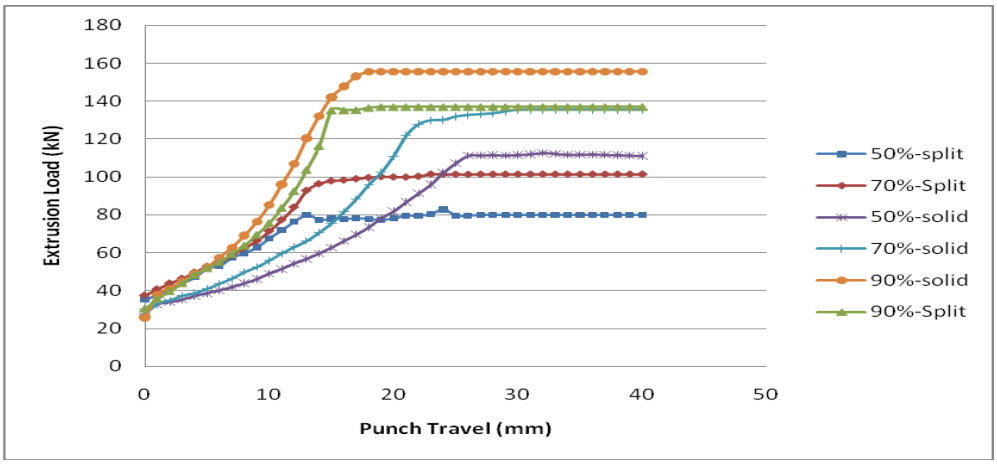

Figure 28. Comparison of extrusion load with punch travel in dry condition for different reduction

The Comparison of variation of extrusion load with respect to the punch travel in lubricated condition for solid workpiece and split workpiece are shown in the fig.28. It is found that the load in case of split workpiece is less than the solid work piece for same reduction whereas the Comparison of variation of extrusion load with respect to the punch travel in lubricated condition for solid workpiece and split workpiece are shown in the fig.29. It is found that the load in case of split workpiece is less than the solid work piece for 50% reduction

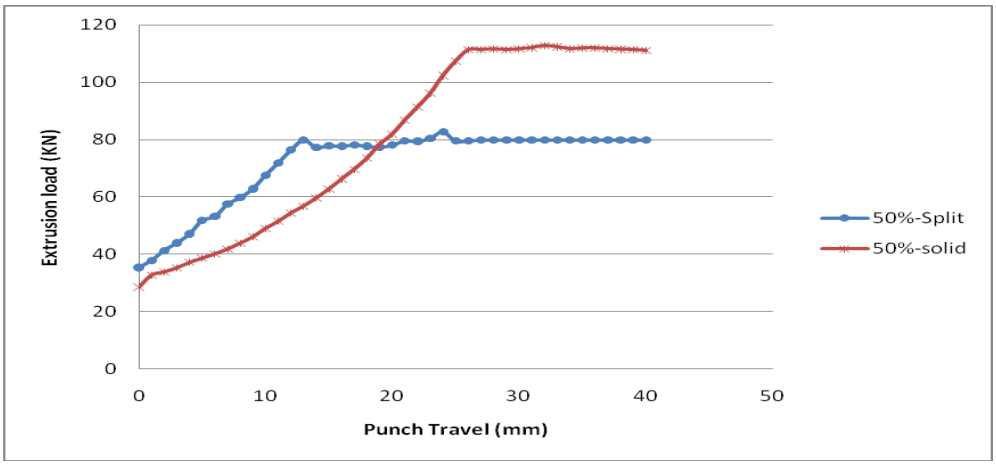

Figure 29. Comparison of extrusion load with punch travel in lubricated condition for solid and split die with 50% reduction

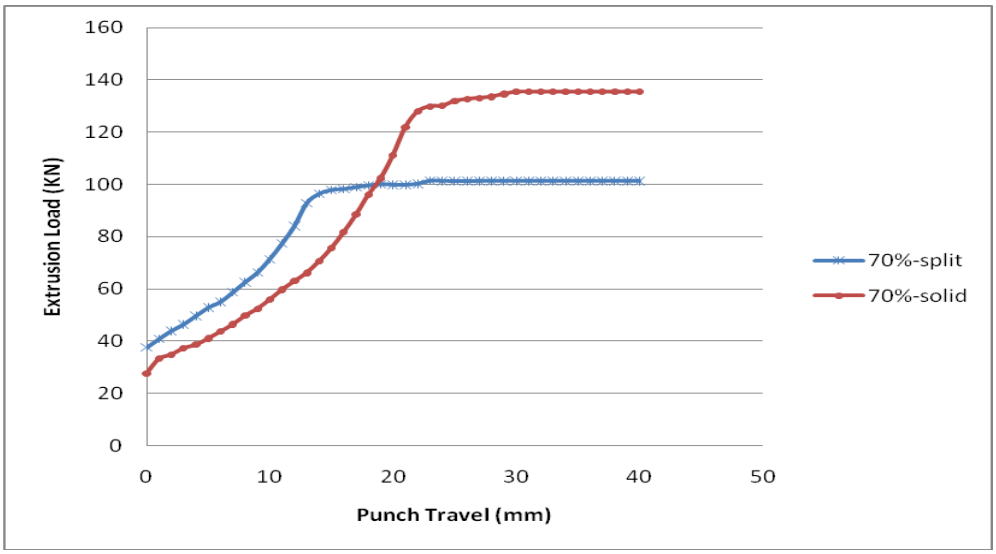

Figure 30. Comparison of extrusion load with punch travel in lubricated condition for solid and split die with 70% reduction

The Comparison of variation of extrusion load with respect to the punch travel in lubricated condition for solid workpiece and split workpiece are shown in the fig.30. It is found that the load in case of split workpiece is less than the solid workpiece for 70% reduction

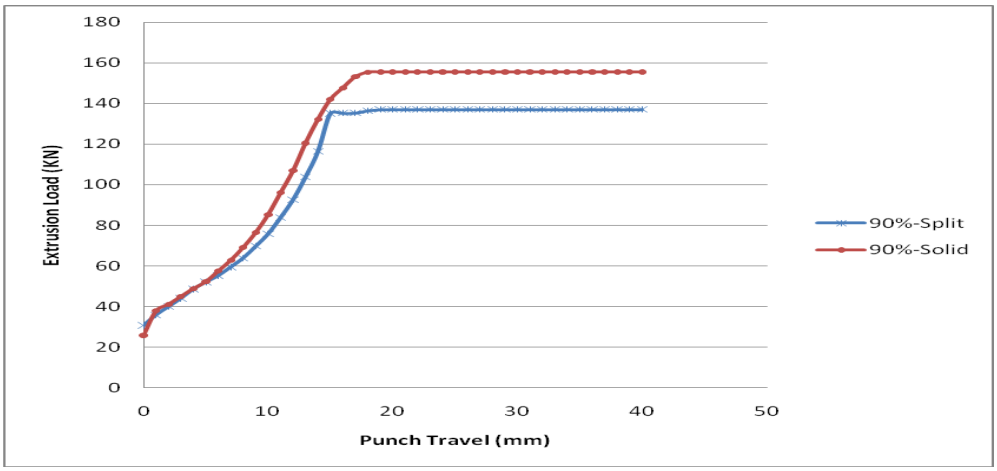

Figure 31.Comparison of extrusion load with punch travel in lubricated condition for solid and split die with 90% reduction

The Comparison of variation of extrusion load with respect to the punch travel in lubricated condition for solid workpiece and split workpiece are shown in the fig.31. It is found that the load in case of split workpiece is less than the solid workpiece for 90% reduction

6.2 FEM simulation of Alluminium-1100

FEM Simulation using aluminum-1100 as work material was done with non-linear converging die (cosine die) and linear converging die. It is found that the extrusion load is less in case of cosine die as shown in fig.32. Some properties like effective stress, velocity and principal stress at last step are shown in fig.33

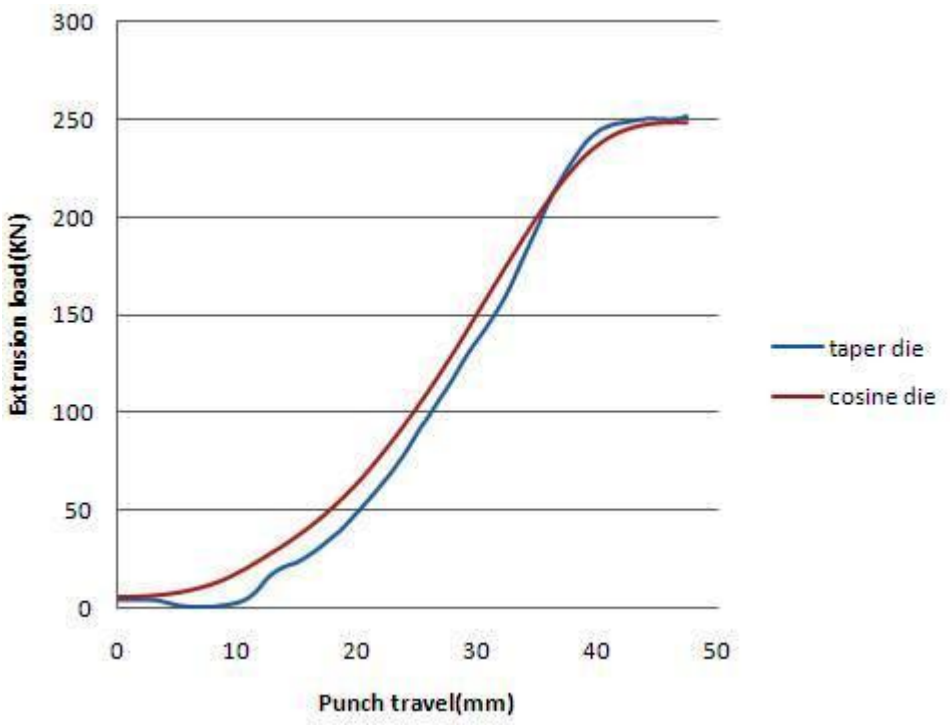

Figure 32.Comparison of extrusion load with punch travel in lubricated condition with cosine and taper die

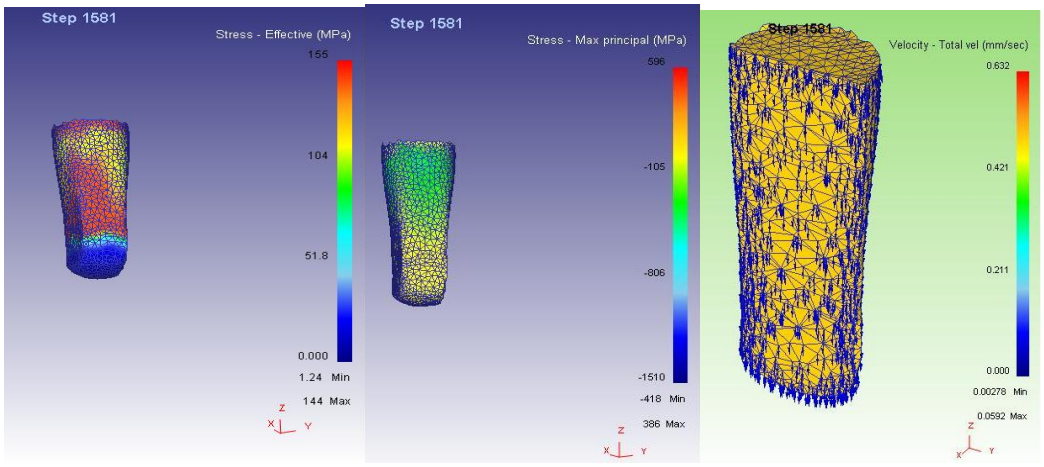

Figure 33. Effective stress, principal stress and velocity field at last step of extrusion

6.2.1 FEM simulation of pure lead

FEM simulation using lead was done for two frictional conditions 0.38 and 0.75 as derived from experiment using ring compression test. Extrusion load with punch travel for friction factor m=0.38 and m= 0.75 are shown in fig .34.

Some properties like velocity and principal stress at last step are shown in fig .35.

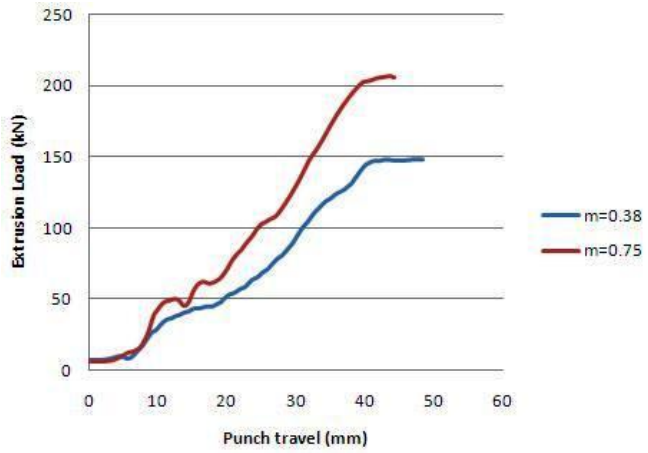

Figure 34. Extrusion load with punch travel for dry and lubricated condition using cosine die

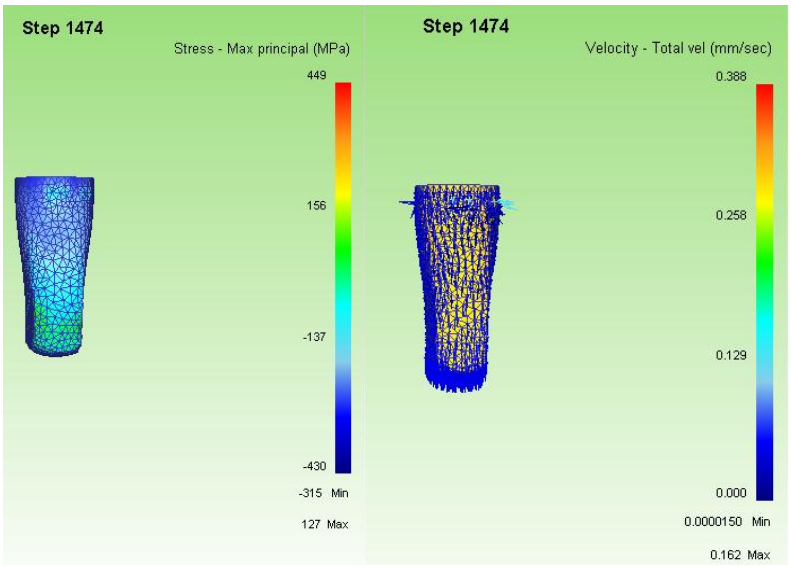

Figure 35. Principal stress and velocity field at last step of extrusion

Chapter 7

CONCLUSIONS

Chapter 7

Conclusions

- A non-linear converging die profile has been designed for extrusion of square section from round billet using cosine function.
- The extrusion load increases with increase in reduction and friction factor.
- Load in case of split test is less as compared to solid work material under same experimental condition.
- The extrusion load for non-linear converging die is less as compared to linear converging die under same simulation condition.
- The flow of material in non-linear converging die appears to be gradual specially in higher reduction

REFERENCES

[1] S.K. Sahoo, P.K. Kar, K.C. Singh, A numerical application of the upper-bound technique for round-to-hexagon extrusion through linearly converging dies, Journal of Materials Processing Technology 91 (1999) 105–110

[2] S.K. Sahoo, P.K. Kar, K.C. Singh, Upper-bound analysis of the extrusion of a bar of channel section from square/rectangular billets through square dies, Journal of Materials Processing Technology 75 (1998) 75–80

[3] K.P. Maity, P.K. Kar, N.S**.** Das, A class of upper-bound solutions for the extrusion of square Shapes from square billets through curved dies, Journal of Materials Processing Technology 62 (1996) 185- 190

[4] R. Narayanasamy, R. Ponalagusamy, R. Venkatesan, P. Srinivasan, An upper bound solution to extrusion of circular billet to circular shape through cosine dies, Materials and Design 27 (2006) 411–415

[5] R.K. Sahoo, P.K. Kar, S.K. Sahoo, 3D upper-bound modeling for round-to-triangle section extrusion using the SERR technique, Journal of Materials Processing Technology 138 (2003) 499–504

[6] B.S. Altan, G. Purcek, I. Miskioglu, An upper-bound analysis for equal-channel angular extrusion, Journal of Materials Processing Technology 168 (2005) 137–146

[7] J.S. Ajiboye, M.B. Adeyemi , Upper bound analysis of die land length in cold extrusion, Journal of Materials Processing Technology 177 (2006) 608–611

[8] M.H. Paydara, M. Reihaniana, R. Ebrahimia, T.A. Deanb, M.M. Moshksara, An upper-bound approach for equal channel angular extrusion with circular cross-section, journal of materials processing technology 198 (2008) 48–53

[9] D.K. Kim, J.R. Cho, W.B. Bae, Y.H. Kim, Upper-bound analysis of square-die forward extrusion, Journal of Materials Processing Technology 62 (1996) 242 - 248

[10] S.K. Sahoo, Comparison of SERR analysis in extrusion with experiment, Journal of Materials Processing Technology 103 (2000) 293-303

[11] Y.H. Kim, J.R. Choa, K.S. Kim, H.S. Jeong, S.S. Yoon, A study of the application of upper bound method to the CONFORM process, Journal of Materials Processing Technology 97 (2000) 153-157

[12] W.A. Gordon, C.J. Van Tyne, Y.H. Moon, Overview of adaptable die design for extrusions, Journal of Materials Processing Technology 187–188 (2007) 662–667

[13] N. Venkata Reddy, R. Sethurama, G.K. Lal, Upper-bound and finite-element analysis of axisymmetric hot extrusion, Journal of Materials Processing Technology 57 (1996) 14 22

[14] M.K. Sinha, S. Deb, U.S. Dixit, Design of a multi-hole extrusion process, Materials and Design 30 (2009) 330–334

[15] W. Johnson, Experiments in the cold extrusion of rods of non-circular sections, Journal of Mechanics and Physics of Solids 7 (1958) 37-44.

[16] K. P. Maity, A. K. Rout, Kalu Majhi, computer-aided simulation of metal flow through curved die for extrusion of square section from square billet , Presented in International Conference on Extrusion and Benchmark, Dortmund, Germany, 16-17 September, 2009

[17] B.B. Basily, D.H. Sansome, Some theoretical considerations for the direct drawing of section rod from round bar, Int. J. Mech. Sci. 18 (1979) 201–209

[18] V. Nagpal, T. Altan, Analysis of the three-dimensional metal flow in extrusion of shapes. With the use of dual stream function, in: Proceedings of the Third North American Metal Research Conference, Pittsburgh, PA, 1975, pp. 26–40

[19] D.Y. Yang, C.H. Lee**,** Analysis of three-dimensional extrusion of sections through curved dies by conformal transformations, International Journal of mechanical science 20 (1978) 541–552

[20] R. Prakash, O.H. Khan, An analysis of plastic flow through polygonal converging dies with generalized boundaries of the zone of plastic deformation, Int. J. Mach. Tool Des. Res. 19 (1979)1–9.

[21] F. Gatto, A. Giarda, The characteristics of three-dimensional analysis of plastic deformation according to the SERR method, Int. J. Mech. Sci. 23 (1981) 129–148.

[22] F. Halvorsen, T. Aukrust, Studies of the mechanisms for buckling and waving in aluminum extrusion by use of a Lagrangian FEM software, International Journal of Plasticity 22 (2006) 158–173

[23] J. Lof, Y. Blokhuis, FEM simulations of the extrusion of complex thin-walled aluminium sections, Journal of Materials Processing Technology 122 (2002) 344–354

[24] LIU Gang, ZHOU Jie, J DUSZCZYK, Process optimization diagram based on FEM simulation for extrusion of AZ31 profile, Trans. Nonferrous met. Soc. china18 (2008) 247-251

[25] Tapas chanda, Jie zbou, Jurek Duszczyk, A comparative study on iso-speed extrusion and isothermal extrusion of 6061 Al alloy using 3D FEM simulation, Journal of Material Processing Technology 114 (2001) 145-153

[26] T. Chanda, J. Zhou, J. Duszczyk, FEM analysis of aluminium extrusion through square and round dies , Materials and Design 21 (2000) 323-335

[27] Zhong Hu, Lihua Zhu, Benyi Wang, Zhuang Liu, Yongchun Miao,Peiliang Xie, Shengxing Gu, Wei Sheng, Computer simulation of the deep extrusion of a thin-walled cup using the thermo-mechanically coupled elasto-plastic FEM, Journal of Materials Processing Technology 102 (2000) 128-137

[28] K. D. Bouzakis, K. Efstathiou, G. Paradisiadis, A. Tsouknidas, Experimental and FEM-supported investigation of wet ceramic clay extrusion for the determination of stress distributions on the applied tools' surfaces, Journal of the European Ceramic Society 28 (2008) 2117–2127

[29] Q. Li, C.J. Smith, C. Harris, M.R. Jolly, Finite element investigations upon the influence of pocket die designs on metal flow in aluminium extrusion Part I. Effect of pocket angle and volume on metal flow, Journal of Materials Processing Technology 135 (2003) 189–196

[30] Zhi Peng, Terry Sheppard, Simulation of multi-hole die extrusion, Materials Science and Engineering A 367 (2004) 329–342

[31] *Gang Fang, Jie Zhou, Jurek Duszczy* ,FEM simulation of aluminium extrusion through two-hole multi-step pocket dies,journal of materials processing technology 209 (2009) 1891–1900

[32] Xinjian Duana, X. Velay, T. Sheppard, Application of finite element method in the hot extrusion of aluminium alloys, Materials Science and Engineering A369 (2004) 66–75

[33] Geun-An Lee, Yong-Taek Im, Analysis and die design of at-die hot extrusion process 2. Numerical design of bearing lengths, International Journal of Mechanical Sciences 44 (2002) 935–946